IEEE Access
Multidisciplinary | Rapid Review | Open Access Journal

Received 28 January 2023, accepted 5 February 2023, date of publication 9 February 2023, date of current version 17 February 2023.

*Digital Object Identifier 10.1109/ACCESS.2023.3243662*

RESEARCH ARTICLE

# A Joint Optimization Model for Transmission Capacity and Wind Power Investment Considering System Security

**AHMAD M. ALSHAMRANI[1], MOHAMMED A. EL-MELIGY[2], MOHAMED ABDEL FATTAH SHARAF[2], AND EMAD ABOUEL NASR[2]**

[1]Statistics and Operations Research Department, College of Science, King Saud University, Riyadh 11451, Saudi Arabia
[2]Industrial Engineering Department, College of Engineering, King Saud University, Riyadh 11421, Saudi Arabia

Corresponding author: Mohamed Abdel Fattah Sharaf (mfsharaf@ksu.edu.sa)

This work was supported by the Deputyship for Research and Innovation, Ministry of Education, Saudi Arabia, under Project IFKSURG-2-1587.

**ABSTRACT** Due to continuous growth in electric demand and increasing connection of renewable energy, the power systems are being operated with smaller stability margins. Therefore, a sufficient loading margin is essential to maintain the system secure and ensure voltage stability. To this end, this paper studies the joint optimization of transmission capacity and wind power investment problem, the unique feature of which is incorporating voltage stability margin (VSM) in the planning model. A bi-level model has been formulated whose upper level minimizes the total investment and operation cost minus the weighted VSM. The lower level evaluates the VSM given the optimal expansion plan from the upper level. In addition, the stochastic nature of wind power and load can impact voltage stability. Thus, uncertainties related to intermittent wind generation and demand must be modeled. We use an approximated linear representation to model the AC power system at both levels of the problem. The duality theory (primal-dual formulation) is utilized to transform bi-level programming into single-level mathematical programming. The validity of the constructed methodology is demonstrated on the IEEE 24-bus RTS, which indicates the efficacy and feasibility of the presented model.

**INDEX TERMS** Bi-level programming, primal-dual formulation, transmission and wind investment, voltage stability.

## NOMENCLATURE

### A. INDICES AND SETS

| | |
|---|---|
| $\Omega^N$ | Set of buses indexed by $i, j$. |
| $\Omega^S$ | Set of scenarios indexed by $s$. |

### B. PARAMETERS

| | |
|---|---|
| $g_{ij}, b_{ij}$ | Conductance and susceptance of a transmission line. |
| $A_k, B_k, C$ | Constant parameters used to approximate a circle by a regular polygon. |
| $a_i^T, b_i^T, c_i^T$ | Production cost coefficients of a thermal unit. |
| $I_i^W, I_{ij}^L$ | Annualized investment cost of a wind farm and a transmission line. |
| $M_1, M_2, M_3, M_4$ | Big-M parameters. |
| $P_{is}^{D0}$ | Active power demand. |
| $Q_{is}^{D0}$ | Reactive power demand. |
| $\overline{S}_{ij}^L$ | Capacity of a line. |
| $\overline{P}_i^T$ | Maximum active power generation of a thermal power plant. |
| $\underline{Q}_i^T, \overline{Q}_i^T$ | Minimum and maximum reactive power generation of a thermal power plant. |
| $K_i^G$ | A variable to model the distributed slack bus. |

The associate editor coordinating the review of this manuscript and approving it for publication was Ehab Elsayed Elattar.

| | |
|---|---|
| $N_s$ | Number of hours in scenario $s$. |
| $\underline{\Delta v_i}$, $\overline{\Delta v_i}$ | Minimum and maximum voltage deviation. |
| $\underline{\delta_i}$, $\overline{\delta_i}$ | Minimum and maximum voltage angle. |
| $\pi_{is}$ | Capacity factor of a wind farm ($0 \leq \pi_{is} \leq 1$). |
| $\Lambda$ | Weighting coefficient. |

### C. VARIABLES

| | |
|---|---|
| $P^L_{ijs} \tilde{P}^L_{ijs} P^{L0}_{ijs}$ | Lines' active power flow in the main problem, VSM assessment problem and OPF problem. |
| $Q^L_{ijs} \tilde{Q}^L_{ijs} Q^{L0}_{ijs}$ | Lines' reactive power flow in the main problem, VSM assessment problem and OPF problem. |
| $LF_s$ | Loading factor. |
| $\tilde{P}^D_{is}$ | Active power demand in the VSM assessment problem. |
| $\tilde{Q}^D_{is}$ | Reactive power demand in the VSM assessment problem. |
| $P^T_{is}$, $\tilde{P}^T_{is}$, $P^{T0}_{is}$ | Active power generation of thermal units in the main problem, VSM assessment problem and OPF problem. |
| $Q^T_{is}$, $\tilde{Q}^T_{is}$, $Q^{T0}_{is}$ | Reactive power generation of thermal units in the main problem, VSM assessment problem and OPF problem. |
| $P^W_{is}$, $\tilde{P}^W_{is}$, $P^{W0}_{is}$ | Active power generation of wind farms in the main problem, VSM assessment problem and OPF problem. |
| $Q^W_{is}$, $\tilde{Q}^W_{is}$ $Q^{W0}_{is}$ | Reactive power generation of wind farms in the main problem, VSM assessment problem and OPF problem. |
| $\overline{P}^W_i$ | Capacity of a wind farm. |
| $u^L_{ij}$ | Binary variable indicating the installation status of a transmission line. |
| $\Delta v_{is}$, $\Delta \tilde{v}_{is}$, $\Delta v^0_{is}$ | Voltage deviation in the main problem, VSM assessment problem and OPF problem. |
| $\delta_{is}$, $\tilde{\delta}_{is}$ $\delta^0_{is}$ | Voltage angle in the main problem, VSM assessment problem and OPF problem. |
| $\delta_{ref,s}$ | Voltage angle at the reference bus. |

## I. INTRODUCTION

### A. BACKGROUND, MOTIVATION, AND CONTRIBUTION

Current power grids are being utilized with smaller stability margins due to continuous growth in electric demand and the integration of renewable energy sources (RES). As a result, the power systems are more likely to become unstable due to voltage instability. Voltage stability studies have attained great attention since voltage collapse makes the power system insecure and may lead to significant economic losses. It is responsible for a number of blackouts throughout the world and harms social welfare and industrial activities. Thus, voltage stability evaluation is vital for power system planning and operation.

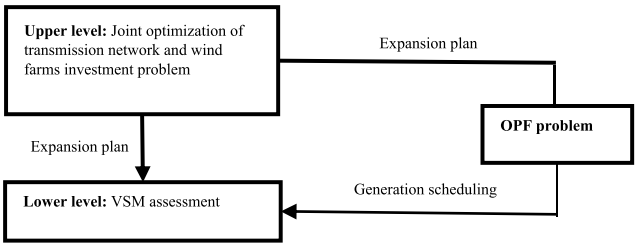


**FIGURE 1.** A representation scheme of the presented investment model.

In this study, we investigate the joint optimization problem of transmission capacity and wind power investment considering voltage stability. Hence, it is necessary to include the voltage stability margin (VSM) in the investment planning process. The VSM is a widely used index to measure voltage stability in literature, showing the maximum load growth a power system can tolerate in the existing operating condition [1], [2]. In this context, a bi-level structure is established for the investment problem under uncertainty. The first level addresses the planning problem seeking to minimize the total investment and operation cost while maximizing VSM subject to the technical limitations of the power system. With the optimal expansion plan acquired from the first level, the second level calculates the VSM of the system. An approximated linear network model for AC power flow equations is employed at both levels. The primal-dual formulation is used to solve this bi-level programming. In doing so, the second level is replaced by the primal and dual feasibility constraints and the strong duality equality.

In addition, the penetration level of RESs in the power grid has been escalated to decrease greenhouse gas emissions and dependence on diminishing fossil fuels. On the other hand, increasing energy prices have pushed governments to design new policies to decarbonize energy production. Hence, RESs play a vital role in the modern power grid, such that 62% of the total installed capacity between 2009 and 2018 [3] is green energy. However, the RESs are expected to be expanded four times faster than before from now to 2030 to alleviate the impact of climate change [3]. The most popular RES is wind energy, the fastest-growing technology in generating electric power. The inherent stochastic nature of generated wind power can greatly influence voltage stability. Thus, intermittent wind power generation and uncertainties related to the load demand must be modeled to gain an insightful understanding of VSM with high wind energy penetration.

The existing literature on the planning studies does not model the voltage stability effect on the transmission network and wind power investment problem. Instead, economic

approaches with prevailing power system constraints have been established while ignoring voltage stability. These approaches do not bring an insightful view of the effect of planning results on voltage stability. However, the development of existing models is required to compute the proximity of an operating state to a voltage instability when deciding to expand and reinforce an existing transmission network with a high share of wind power generation. In this respect, the contribution of this paper is established by presenting a novel strategy for the investment problem of transmission and wind power while modeling the VSM. The purpose of the proposed method is to minimize the total investment and operation cost while maximizing the maximum loadability of an electric power grid. The entire proposed expansion planning process is illustrated in Fig. 1.

### B. LITERATURE REVIEW

A novel transmission expansion planning (TEP) framework to guarantee that the power system is robust under conditions with high demand and low production of RES is presented in [4], where a comprehensive comparison between the widely-used decision-making models is provided. A non-deterministic TEP model, including distributed series reactors, is proposed by [5], where the Monte Carlo simulation method is used to model the uncertainty of wind power and electric demands. Reference [6] constructs an offshore transmission network expansion model for large-scale wind connection to the grid allowing the planners to assess the techno-economic feasibility of several potential options under various uncertainties. An innovative co-optimization model for investment in wind power, energy storage systems (ESSs), and transmission lines is formulated in [7], which considers transmission switching and unit commitment constraints. A multi-period multi-objective generation and transmission expansion planning with demand response (DR) is jointly modeled in [8] to obtain an optimal expansion plan, where several levels of DR penetration in the planning system are considered. Reference [9] proposes a stochastic transmission investment model considering the dynamic thermal rating of overhead lines, in which the objective function includes operational costs and the investment costs of line and dynamic thermal rating installation. A multi-stage TEP model is proposed in [10] considering the high voltage AC and DC alternatives (HVAC and HVDC), where the possibility of converting existing HVAC lines to HVDC lines is modeled in the presence of high shares of RES and ESS. Reference [11] presents a linearized AC model for coordinated TEP and reactive power planning considering wind power investment, where a special ordered set of type 2 is employed to make the model linear. A multi-objective model which determines the optimal expansion planning for generation and transmission is set out in [12]. The objective function is to minimize the investment costs of the new wind farms, new lines, fuel costs, and emissions, as well as to maximize incentives for new generating units. The effect of wind speed's spatial distribution on the joint generation and transmission expansion planning, including wind farms, is studied in [13], and it is verified that ignoring wind speed's spatial distribution impacts the expected exploitable wind power. Reference [14] suggests a security-constrained co-planning of transmission expansion and ESS in a wind-integrated power system. The problem is formulated as mixed-integer linear programming (MILP) and is solved by Benders decomposition. Reference [15] develops an efficient, two-stage method for security-constrained TEP using AC power flow, where a modified artificial bee colony algorithm is employed to solve the optimization problem. To overcome the disadvantages of conventional robust approaches in the transmission investment problem, Reference [16] establishes a novel strategy by modeling the probability of renewable power generation uncertainty. In this sense, a hybrid probability uncertainty set is constructed using 1-norm and $\infty$-norm metrics [16]. A robust optimization model for ESS and transmission line investment co-planning, considering binary variables related to ESS statuses in the recourse problem, is established in [17], where an enhanced nested column and constraint generation technique is used to solve the problem. A scenario-based AC transmission investment model is put forth in [18], where combinations of load, wind, and N-1 contingency uncertainties are assessed with Monte Carlo simulation and the loading limits for the existing and candidate lines. A stochastic transmission and generation expansion planning model is formulated in [19] to increase the hosting capacity of networks and satisfy future load demands, in which two algorithms, namely, the weighted mean of vectors optimization and sine cosine algorithms, are used to solve the problem. Reference [20] presents a distributionally robust optimization-based planning scheme considering load and wind uncertainties from the data-driven ambiguity set. Besides generating units and transmission lines, DR and solar power plants are also modeled as investment options. Reference [21] proposes a scenario-driven probabilistic framework to assess the impact of intermittent wind power on the TEP problem. Authors in [22] develop a solution algorithm to cope with the robust transmission line investment planning where the lower level is replaced by its dual. The authors claim that neither binary variables nor bilinear terms are introduced in this approach. Some spatial and temporal simplifications is proposed to the expansion planning problem of the generation and transmission in [23], where three formulations, i.e., a big-M formulation, a hull formulation, and an alternative big-M formulation, are compared. Authors in [24] constructs an investment planning model that finds an optimal mix of transmission-level non-generation flexible assets: ESS, thyristor-controlled series compensators (TCSC), and transmission lines. A new model with several expansion plans that operate efficiently in all the previously defined generation scenarios is developed in [25], allowing the planner to find adequate expansion plans. An efficient MILP method is formulated in [26] to solve the dynamic contingency-constrained TEP problem, where an iterative algorithm based on line outage distribution factors screens the worst-case contingency. A two-stage

Internet data center (IDC)-considered scheme in generation and transmission network expansion planning is presented in [27] to make full use of IDCs' spatial and chronological load regulation potentials for DR. A robust method for coordinated transmission and energy storage expansion planning in wind -integrated power grids is introduced in [28] considering wind and demand uncertainty. Reference [29] addresses the question of how large the uncertainty set should be in the transmission expansion planning problem and optimizes the value of the uncertainty budget.

The rest of this study is outlined as follows. Section II formulates the joint transmission and wind investment model, while VSM is included in the planning problem. The solution technique is explained in Section III. A case study is demonstrated in Section IV to validate the effectiveness of the proposed method. Section V provides several concluding remarks.

## II. PROBLEM STATEMENT

This section contains two subsections. The mathematical model to evaluate VSM is provided in subsection II-A. Then, the scenario-driven expansion planning model for investing in transmission and wind is devised in subsection II-B.

### A. VOLTAGE STABILITY MARGIN EVALUATION

The VSM gives an intuitive indicator of the loadability margin of a power grid. It shows the extra power consumption that will lead to a voltage collapse. Reference [30] uses a novel optimization model for the power system's voltage stability and harmonic analysis. A voltage stability indicator incorporating voltage-dependent load is formulated in [31]. The voltage stability margin is computed in power grids using a modal analysis in [32] by calculating a specified number of the smallest eigenvalues. An integrated framework is presented in [33] to determine the VSM using correlation detection and random bits forest. In [34], unstable areas in integrated transmission-distribution grids are identified regarding voltage stability and maximum loadability. A voltage stability index is presented in [35] based on the P-V curve, where the voltage stability index is computed in terms of the distance between the operating point and saddle point on the P-V curve. A control model for static voltage stability considering the interval uncertainty of wind power output is suggested by [36], where the objective functions are to increase the central value and decrease the fluctuation range. Based on the models presented in the literature, the VSM in scenario $s$ for a given investment plan can be computed as follows:

$$\underbrace{\text{Maximize}}_{\tilde{P}^T_{is},\tilde{Q}^T_{is},\tilde{P}^W_{is},\tilde{Q}^W_{is},\tilde{P}^D_{is},\tilde{Q}^D_{is},\tilde{P}^L_{ijs},\tilde{Q}^L_{ijs},\Delta\tilde{v}_{is},\tilde{\delta}_{is},L\ F_s} \quad LF_s \tag{1}$$

$$\text{subject to: } \underbrace{P^{T0}_{is}\left(1+LF_s+K^G_i\right)}_{P^T_{is}} + \underbrace{P^{W0}_{is}\left(1+LF_s+K^G_i\right)}_{\tilde{P}^W_{is}} - \sum_j \tilde{P}^L_{ijs}$$

$$= \underbrace{P^{D0}_{is}\left(1+LF_s\right)}_{P^D_{is}} < \chi^{BP}_{is} > \tag{2}$$

$$\tilde{Q}^T_{is} + \tilde{Q}^W_{is} - \sum_j \tilde{Q}^L_{ijs} =< \chi^{BQ}_{is} > \tag{3}$$

$$\tilde{P}^L_{ijs} = u^L_{ij}\left(g_{ij}\left(\Delta\tilde{v}_{is}-\Delta\tilde{v}_{js}\right) - b_{ij}\left(\tilde{\delta}_{is}-\tilde{\delta}_{js}\right)\right) < \chi^{LP}_{ijs} > \tag{4}$$

$$\tilde{Q}^L_{ijs} = u^L_{ij}\left(-b_{ij}\left(\Delta\tilde{v}_{is}-\Delta\tilde{v}_{js}\right) - g_{ij}\left(\tilde{\delta}_{is}-\tilde{\delta}_{js}\right)\right) < \chi^{LQ}_{ijs} > \tag{5}$$

$$0 \le P^{T0}_{is}\left(1+LF_s+K^G_i\right) \le \overline{P}^T_i < \underline{\chi}^{TP}_{is}, \overline{\chi}^{TP}_{is} > \tag{6}$$

$$\underline{Q}^T_i \le \tilde{Q}^T_{is} \le \overline{Q}^T_i < \underline{\chi}^{TQ}_{is}, \overline{\chi}^{TQ}_{is} > \tag{7}$$

$$0 \le P^{W0}_{is}\left(1+LF_s+K^G_i\right) \le \pi_{is}\overline{P}^W_i < \underline{\chi}^{WP}_{is}, \overline{\chi}^{WP}_{is} > \tag{8}$$

$$\pi_{is}\underline{Q}^W_i \le Q^W_{is} \le \pi_{is}\overline{Q}^W_i < \underline{\chi}^{WQ}_{is}, \overline{\chi}^{WQ}_{is} > \tag{9}$$

$$A_k\tilde{P}^L_{ijs} + B_k\tilde{Q}^L_{ijs} \le C\overline{S}^L_{ij} < \chi^L_{ijks} > \tag{10}$$

$$\underline{\Delta v}_i \le \Delta\tilde{v}_{is} \le \overline{\Delta v}_i < \underline{\chi}^v_{is}, \overline{\chi}^v_{is} > \tag{11}$$

$$\underline{\delta}_i \le \tilde{\delta}_{is} \le \overline{\delta}_i < \underline{\chi}^{\delta}_{is}, \overline{\chi}^{\delta}_{is} > \tag{12}$$

$$\delta_{ref,s} = 0 < \chi^{\delta}_{ref,s} > \tag{13}$$

Eq. (1) is the second level's objective function. Eqs. (2) and (3) enforce the active and reactive power balance where $K^G_i$ is used to model a distributed slack bus. Eqs. (4) and (5) are the active and reactive power that flow through each transmission line. Active and reactive power produced by thermal and wind generators are restricted by Eqs. (6)-(9). The capacity of each line is limited by Eq. (10). Eqs. (11)-(12) bound the voltage magnitude deviation and voltage angle. Eq. (13) fixes the voltage angle at the slack bus to zero. The variables in front of each equation are corresponding dual variables of the VSM problem defined as the following set:

$$\left\{ \begin{array}{l} \chi^{BP}_{is}, \chi^{BQ}_{is}, \chi^{LP}_{ijs}, \chi^{LQ}_{ijs}, \underline{\chi}^{TP}_{is}, \overline{\chi}^{TP}_{is}, \chi^{TQ}_{is}, \overline{\chi}^{TQ}_{is}, \underline{\chi}^{WP}_{is}, \overline{\chi}^{WP}_{is}, \\ \underline{\chi}^{WQ}_{is}, \overline{\chi}^{WQ}_{is}, \chi^{L}_{ijks}, \underline{\chi}^{v}_{is}, \overline{\chi}^{v}_{is}, \underline{\chi}^{\delta}_{is}, \overline{\chi}^{\delta}_{is}, \chi^{\delta}_{ref,s} \end{array} \right\}$$

It should be highlighted that Eq. (4) is a linear version of the following nonlinear exact form:

$$\tilde{P}^L_{ijs} = u^L_{ij}\left(g_{ij}\left(\tilde{v}_{is}\right)^2 - \tilde{v}_{is}\tilde{v}_{js}\left(g_{ij}\times cos\left(\tilde{\delta}_{is}-\tilde{\delta}_{js}\right) + b_{ij}\times sin\left(\tilde{\delta}_{is}-\tilde{\delta}_{js}\right)\right)\right) \tag{14}$$

By assuming $\tilde{v}_{is} = 1+\Delta\tilde{v}_{is}$ and $\tilde{v}_{js} = 1+\Delta\tilde{v}_{js}$, substituting in Eq. 14 and ignoring higher order terms, we obtain [37]:

$$\tilde{P}^L_{ijs} = u^L_{ij}\left(g_{ij}\left(\Delta\tilde{v}_{is} - \Delta\tilde{v}_{js}\right) - b_{ij}\left(\tilde{\delta}_{is} - \tilde{\delta}_{js}\right)\right) \quad (15)$$

The same approach can be carried out to acquire Eq. (5).

### B. BI-LEVEL MODEL FOR TRANSMISSION AND WIND POWER EXPANSION PLANNING CONSIDERING VSM

In the first level of the proposed bi-level structure, the total investment and operation cost is minimized while maximizing the VSM. With the optimal investment plan acquired from the first level, the second level is activated to calculate the VSM. The whole bi-level structure is formulated as below:

$$\underbrace{\text{Minimize}}_{P_{is},Q^T_{is},P^T_{is},Q^W_{iS},P^L_{ijs'},Q^L_{ijs'},\Delta v_{is},\delta_{is}\bar{P}^W_i,u^L_{ij}} \sum_{(ij)} I^L_{ij}u^L_{ij} + \sum_i I^W_i\overline{P}^W_i + \sum_s N_s\sum_i\left(a^T_i\left(P^T_{is}\right)^2 + b^T_i P^T_{is} + c^T_i\right) - \Lambda\sum_s N_s LF_s \quad (16)$$

$$\text{subject to: } P^T_{is} + P^W_{is} - \sum_j P^L_{ijs} = P^{D0}_{is} \quad (17)$$

$$Q^T_{is} + Q^W_{is} - \sum_j Q^L_{ijs} = Q^{D0}_{is} \quad (18)$$

$$-\left(1-u^L_{ij}\right)M_1 \le P^L_{ijs} - \left(g_{ij}\left(\Delta v_{is} - \Delta v_{js}\right) - b_{ij}\left(\delta_{is} - \delta_{js}\right)\right) \le \left(1-u^L_{ij}\right)M_1 \quad (19)$$

$$-\left(1-u^L_{ij}\right)M_2 \le Q^L_{ijs} - \left(-b_{ij}\left(\Delta v_{is} - \Delta v_{js}\right) - g_{ij}\left(\delta_{is} - \delta_{js}\right)\right) \le \left(1-u^L_{ij}\right)M_2 \quad (20)$$

$$0 \le P^T_{is} \le \overline{P}^T_i \quad (21)$$

$$\underline{Q}^T_i \le Q^T_{is} \le \overline{Q}^T_i \quad (22)$$

$$0 \le P^W_{is} \le \pi_{is}\overline{P}^W_i \quad (23)$$

$$\pi_{is}\underline{Q}^W_i \le Q^W_{is} \le \pi_{is}\overline{Q}^W_i \quad (24)$$

$$A_k P^L_{ijs} + B_k Q^L_{ijs} \le C\overline{S}^L_{ij} \quad (25)$$

$$-u^L_{ij}\times M_3 \le P^L_{ijs} \le u^L_{ij}\times M_3 \quad (26)$$

$$-u^L_{ij}\times M_4 \le Q^L_{ijs} \le u^L_{ij}\times M_4 \quad (27)$$

$$\underline{\Delta v}_i \le \Delta v_{is} \le \overline{\Delta v}_i \quad (28)$$

$$\underline{\delta}_i \le \delta_{is} \le \overline{\delta}_i \quad (29)$$

$$\delta_{ref,s} = 0 \quad (30)$$

where

$$LF_s \in \arg\{\underbrace{\text{Maximize}}_{\tilde{P}^T_{is},Q^T_{is},\hat{F}^W_{is},Q^W_{is},\tilde{F}^D_{is},Q^D_{is},\tilde{F}^L_{ijs},Q^L_{ijs},\Delta\tilde{v}_{is},\tilde{\delta}_{is},L\ F_s} LF_s \quad (31)$$

$$\text{subject to: Constraints } (2)-(13) \quad (32)$$

Eq. (16) is the first level's objective function. Eqs. (17)-(18) are the active and reactive power balances. Eqs. (19)-(20) compute each transmission line's active and reactive power flow. The upper and lower bounds for the power generated by thermal and wind units are shown by Eqs. (21)-(24). The capacity of each line is limited by (25). Eqs. (26)-(27) enforce the power flow through a candidate line to be zero if it is not built ($u^L_{ij} = 0$). The voltage angle is limited by Eq. (29). At the reference bus, the voltage angle is forced to be zero by Eq. (30). Eqs. (31)-(32) indicate the second level.

Given the optimal investment plan from the above-formulated problem, the optimal power flow (OPF) is run to obtain the optimal generation scheduling in the base case. Notice that the upper level includes the expected loading factor. Thus, the generation scheduling does not conform to the economic dispatch problem. Hence, it is needed to compute the generation scheduling given the optimal expansion obtained from the upper level. This can be conducted using the optimal power flow as follows:

$$\underbrace{\text{Minimize}}_{P^{T0}_{is},Q^{T0}_{is},P^{W0}_{is},Q^{W0T}_{is},P^{L0}_{ijs'},Q^{L0}_{ijs'},\Delta v^0_{is},\delta^0_{is}} \sum_i a^T_i\left(P^{T0}_{is}\right)^2 + b^T_i P^{T0}_{is} + c^T_i \quad (33)$$

$$\text{subject to: } P^{T0}_{is} + P^{W0}_{is} - \sum_j P^{L0}_{ijs} = P^{D0}_{is} < \chi^{BP0}_{is} > \quad (34)$$

$$Q^{T0}_{is} + Q^{W0}_{is} - \sum_j Q^{L0}_{ijs} = Q^{D0}_{is} < \chi^{BQ0}_{is} > \quad (35)$$

$$P^{L0}_{ijs} = u^L_{ij}\left(g_{ij}\left(\Delta v^0_{is} - \Delta v^0_{js}\right) - b_{ij}\left(\delta^0_{is} - \delta^0_{js}\right)\right) < \chi^{LP0}_{ijs} > \quad (36)$$

$$Q^{L0}_{ijs} = u^L_{ij}\left(-b_{ij}\left(\Delta v^0_{is} - \Delta v^0_{js}\right) - g_{ij}\left(\delta^0_{is} - \delta^0_{js}\right)\right) < \chi^{LQ0}_{ijs} > \quad (37)$$

$$0 \le P^{T0}_{is} \le \overline{P}^T_i < \underline{\chi}^{TP0}_{is}, \overline{\chi}^{TP0}_{is} > \quad (38)$$

$$\underline{Q}^T_i \le Q^{T0}_{is} \le \overline{Q}^T_i < \underline{\chi}^{TQ0}_{is}, \overline{\chi}^{TQ0}_{is} > \quad (39)$$

$$0 \le P^{W0}_{is} \le \pi_{is}\overline{P}^W_i < \underline{\chi}^{WP0}_{is}, \overline{\chi}^{WP0}_{is} > \quad (40)$$

$$\pi_{is}\underline{Q}^W_i \le Q^{W0}_{is} \le \pi_{is}\overline{Q}^W_i < \underline{\chi}^{WQ0}_{is}, \overline{\chi}^{WQ0}_{is} > \quad (41)$$

$$A_k P_{ijs}^{L0} + B_k Q_{ijs}^{L0} \le C\overline{S}_{ij}^{L} < \chi_{ijks}^{L0} > \tag{42}$$

$$\underline{\Delta v}_i \le \Delta v_{is}^{0} \le \overline{\Delta v}_i < \underline{\chi}_{is}^{v0}, \overline{\chi}_{is}^{v0} > \tag{43}$$

$$\underline{\delta}_i \le \delta_{is}^{0} \le \overline{\delta}_i < \underline{\chi}_{is}^{\delta 0}, \overline{\chi}_{is}^{\delta 0} > \tag{44}$$

$$\delta_{ref,s}^{0} = 0 < \chi_{ref,s}^{\delta 0} > \tag{45}$$

These formulations have already been explained. The variables in front of each equation are corresponding dual variables of the OPF problem defined as the following set:

$$\left\{ \begin{array}{l} \chi_{is}^{BP0}, \chi_{is}^{BQ0}, \chi_{ijs}^{LP0}, \chi_{ijs}^{LQ0}, \underline{\chi}_{is}^{TP0}, \overline{\chi}_{is}^{TP0}, \underline{\chi}_{is}^{TQ0}, \overline{\chi}_{is}^{TQ0}, \\ \underline{\chi}_{is}^{WP0}, \overline{\chi}_{is}^{WP0} \underline{\chi}_{is}^{WQ0}, \overline{\chi}_{is}^{WQ0}, \chi_{ijks}^{L0}, \underline{\chi}_{is}^{v0}, \overline{\chi}_{is}^{v0}, \underline{\chi}_{is}^{\delta 0}, \overline{\chi}_{is}^{\delta 0}, \chi_{ref,s}^{\delta 0} \end{array} \right\}$$

The primal-dual formulation of this optimization problem is as below:

$$\text{Eqs.}(35) - (45) \tag{46}$$

$$2a_i^T P_{is}^{T0} + b_i^T + \chi_{is}^{BP0} + \overline{\chi}_{is}^{TP0} - \underline{\chi}_{is}^{TP0} = 0 \tag{47}$$

$$\chi_{is}^{BQ0} + \overline{\chi}_{is}^{TQ0} - \underline{\chi}_{is}^{TQ0} = 0 \tag{48}$$

$$\chi_{is}^{BP0} + \overline{\chi}_{is}^{WP0} - \underline{\chi}_{is}^{WP0} = 0 \tag{49}$$

$$\chi_{is}^{BQ0} + \overline{\chi}_{is}^{WQ0} - \underline{\chi}_{is}^{WQ0} = 0 \tag{50}$$

$$\overline{\chi}_{is}^{\delta 0} - \underline{\chi}_{is}^{\delta 0} + \sum\nolimits_{j\in\Omega^N} u_{ij}^L b_{ij} \left(\chi_{ijs}^{LP0} - \chi_{jis}^{LP0}\right) + u_{ij}^L g_{ij} \left(\chi_{ijs}^{LQ0} - \chi_{jis}^{LQ0}\right) = 0 \tag{51}$$

$$\chi_{ref,s}^{\delta 0} + \sum\nolimits_j \left\{ u_{ij}^L b_{ij} \left(\chi_{ijs}^{LP0} - \chi_{jis}^{LP0}\right) + u_{ij}^L g_{ij} \left(\chi_{ijs}^{LQ0} - \chi_{jis}^{LQ0}\right) \right\} = 0 \tag{52}$$

$$\overline{\chi}_{is}^{v0} - \underline{\chi}_{is}^{v0} + \sum\nolimits_{j\in\Omega^N} u_{ij}^L b_{ij} \left(\chi_{ijs}^{LQ0} - \chi_{jis}^{LQ0}\right) - x_{ij}^L g_{ij} \left(\chi_{ijs}^{LP0} - \chi_{jis}^{LP0}\right) = 0 \tag{53}$$

$$-\chi_{is}^{BP0} + \chi_{ijs}^{LP0} + \sum_k A_k \overline{\chi}_{ijks}^{L0} = 0 \tag{54}$$

$$-\chi_{is}^{BQ0} + \chi_{ijs}^{LQ0} + \sum_k B_k \overline{\chi}_{ijks}^{L0} = 0 \tag{55}$$

$$\underline{\chi}_{is}^{TP0}, \overline{\chi}_{is}^{TP0}, \underline{\chi}_{is}^{TQ0}, \overline{\chi}_{is}^{TQ0}, \underline{\chi}_{is}^{WP0}, \overline{\chi}_{is}^{WP0}, \underline{\chi}_{is}^{WQ0}, \overline{\chi}_{is}^{WQ0}, \chi_{ijks}^{L0}, \underline{\chi}_{is}^{v0}, \overline{\chi}_{is}^{v0}, \underline{\chi}_{is}^{\delta 0}, \overline{\chi}_{is}^{\delta 0}, \chi_{ref,s}^{\delta 0} \ge 0 \tag{56}$$

$$\sum_i c_i^T P_{is}^T = \sum\nolimits_i \left(-P_{is}^{D0} \chi_{is}^{BP0} - Q_{is}^{D0} \chi_{is}^{BQ0} - \overline{P}_i^T \overline{\chi}_{is}^{TP0} - \overline{Q}_i^T \overline{\chi}_{is}^{TQ0} + \underline{Q}_i^T \underline{\chi}_{is}^{TQ0} - \pi_{is} \overline{P}_i^W \overline{\chi}_{is}^{WP0} - \pi_{is} \overline{Q}_i^W \overline{\chi}_{is}^{WQ0} + \pi_{is} \underline{Q}_i^W \underline{\chi}_{is}^{WQ0} - \overline{\Delta v}_i \overline{\chi}_{is}^{v0} + \underline{\Delta v}_i \underline{\chi}_{is}^{v0} - \overline{\delta}_i \overline{\chi}_{is}^{\delta 0} + \underline{\delta}_i \underline{\chi}_{is}^{\delta 0}\right) - \sum\nolimits_{ij} C\overline{S}_{ij}^L \chi_{ijks}^{L0} \tag{57}$$

The primal constraints are shown by Eq. (46). The dual constraints are shown by Eqs. (47)-(56). Eq. 57 shows the strong duality equality. These equations must be added to the upper-level problem to obtain the optimal scheduling in the base case given the solution of the upper level. The solution method is described in the following section.

## III. SOLUTION STRATEGY

The primal-dual formulation is employed to solve the presented bi-level structure. In this regard, the second level It is a well-known technique to use the primal-dual formulation to solve bi-level programming. This technique replaces the second level with its primal (Eq. (61)), dual (Eqs. (62)-(70)), and duality equality constraints (Eq. 71). Hence, the entire problem can be formulated as follows:

$$\underbrace{Minimize} \sum_{(ij)} I_{ij}^L u_{ij}^L + \sum_i I_i^W \overline{P}_i^W + \sum_s N_s \sum_i \left(a_i^T \left(P_{is}^T\right)^2 + b_i^T P_{is}^T + c_i^T\right) - \Lambda \sum_s N_s LF_s \tag{58}$$

subject to: Constraints (17) − (30) (59)

Constraints (46) − (57) (60)

Constraints (2) − (13) (61)

$$\sum\nolimits_i \left(P_{is}^{T0} \chi_{is}^{BP} + P_i^{W0} \chi_{is}^{BP} - P_{is}^{D0} \chi_{is}^{BP} - Q_{is}^{D0} \chi_{is}^{BQ} + P_{is}^{T0} \overline{\chi}_{is}^{TP} - P_{is}^{T0} \underline{\chi}_{is}^{TP} + P_{is}^{W0} \overline{\chi}_{is}^{WP} - P_{is}^{W0} \underline{\chi}_{is}^{WP}\right) = 1 \tag{62}$$

$$\chi_{is}^{BQ} + \overline{\chi}_{is}^{TQ} - \underline{\chi}_{is}^{TQ} = 0 \tag{63}$$

$$\chi_{is}^{BQ} + \overline{\chi}_{is}^{WQ} - \underline{\chi}_{is}^{WQ} = 0 \tag{64}$$

$$\overline{\chi}_{is}^{\delta} - \underline{\chi}_{is}^{\delta} + \sum\nolimits_{j\in\Omega^N} u_{ij}^L b_{ij} \left(\chi_{ijs}^{LP} - \chi_{jis}^{LP}\right) + u_{ij}^L g_{ij} \left(\chi_{ijs}^{LQ} - \chi_{jis}^{LQ}\right) = 0 \tag{65}$$

$$\chi_{ref,s}^{\delta} + \sum\nolimits_j \left\{ u_{ij}^L b_{ij} \left(\chi_{ijs}^{LP} - \chi_{jis}^{LP}\right) + u_{ij}^L g_{ij} \left(\chi_{ijs}^{LQ} - \chi_{jis}^{LQ}\right) \right\} = 0 \tag{66}$$

$$\overline{\chi}_{is}^{v} - \underline{\chi}_{is}^{v} + \sum\nolimits_{j\in\Omega^N} u_{ij}^L b_{ij} \left(\chi_{ijs}^{LQ} - \chi_{jis}^{LQ}\right) - u_{ij}^L g_{ij} \left(\chi_{ijs}^{LP} - \chi_{jis}^{LP}\right) = 0 \tag{67}$$

$$-\chi_{is}^{BP} + \chi_{ijs}^{LP} + \sum_k A_k \overline{\chi}_{ijks}^{L} = 0 \tag{68}$$

$$-\chi_{is}^{BQ} + \chi_{ijs}^{LQ} + \sum_k B_k \overline{\chi}_{ijks}^{L} = 0 \tag{69}$$

$$\underline{\chi}_{is}^{TP}, \overline{\chi}_{is}^{TP}, \underline{\chi}_{is}^{TQ}, \overline{\chi}_{is}^{TQ}, \underline{\chi}_{is}^{WP}, \overline{\chi}_{is}^{WP}, \underline{\chi}_{is}^{WQ}, \overline{\chi}_{is}^{WQ}, \chi_{ijks}^{L}, \underline{\chi}_{is}^{v}, \overline{\chi}_{is}^{v}, \underline{\chi}_{is}^{\delta}, \overline{\chi}_{is}^{\delta}, \chi_{ref,s}^{\delta} \ge 0 \tag{70}$$

$$LF_s = \sum\nolimits_i \left(\chi_{is}^{BP} \left(P_{is}^{D0} - \left(P_{is}^{T0} + P_{is}^{W0}\right)\left(1 + K_i^G\right)\right) + \chi_{is}^{BQ} Q_{is}^{D0} + \overline{\chi}_{is}^{TP} \left(\overline{P}_i^T - P_{is}^{T0}\left(1 + K_i^G\right)\right) + \underline{\chi}_{is}^{TP} \left(P_{is}^{T0}\left(1 + K_i^G\right)\right) + \overline{\chi}_{is}^{WP} \left(\pi_{is} \overline{P}_i^W - P_{is}^{W0}\left(1 + K_i^G\right)\right) + \underline{\chi}_{is}^{WP} \left(P_{is}^{W0}\left(1 + K_i^G\right)\right) + \overline{\chi}_{is}^{TQ} \overline{Q}_i^T - \underline{\chi}_{is}^{TQ} \underline{Q}_i^T$$

$$+\overline{\chi}_{is}^{WQ}\pi_{is}\overline{Q}_i^W - \underline{\chi}_{is}^{WQ}\pi_{is}\underline{Q}_i^W + \overline{\chi}_{is}^{v}\overline{\Delta v}_i - \underline{\chi}_{is}^{v}\underline{\Delta v}_i + \overline{\delta}_i\overline{\eta}_{is}^{\delta} - \underline{\delta}_i\underline{\eta}_{is}^{\delta}\Big) + \sum\nolimits_{ij}\chi_{ijks}^{L}C\overline{S}_{ij}^{L} \quad (71)$$

The above-formulated problem is mixed-integer nonlinear programming (MINLP) due to the presence of bilinear terms. Hence, an MINLP solver must be utilized to solve the program. What follows in section IV shows the implementation of the proposed technique. It is of note that MINLP models suffer from the heavy computational burden for large power grids. In these cases, decomposition techniques can be applied to acquire the optimal solution.

## IV. SIMULATION STUDIES

The model's successful implementation on the IEEE 24-bus RTS is illustrated in this section. All the procedures were coded in KNITRO [38] under GAMS [39]. The experiment is conducted on a computer running at 2.5 gigahertz with 16 gigabytes of RAM. The IEEE 24-bus RTS comprises 10 power plants (32 units) and 38 lines. Candidate wind power plants are located at buses 15, 16, 18, 19, 20, 21, 22, 23, and 24 in which at most 500 MW can be installed at each bus. Existing wind farms are located at buses 14 and 17. Electric load and generator capacity are multiplied by 1.7. Annualized wind investment cost is supposed to be $I_i^W = 120\ 000$ \$/MW. Input data are accessible at [40] for reproducibility purposes. Twenty scenarios are considered to model wind-demand uncertainty. The optimal expansion plan and the related costs are shown in Table 1 for cases (a), and (b), where case (a) indicates the results when the VSM is included in the planning process, and case (b) indicates when VSM is not included. Weighting factor is set to 50000.

It is inferred from the results in Table 1 that optimal expansion scheme for cases (a) and (b) are different. The total cost in case (a) is 5.5% higher than in case (b). However, the loading factor (LF) in case (a) is 15.7% larger than that in case (b). This result points to the effectiveness of the formulated methodology on enhancing the voltage stability. The VSM for each scenario ($LF_s$) of both cases (a) and (b) is depicted in Fig. 2. As illustrated in Fig. 2, loading factor in case (a) is generally larger than the LF in case (b) showing the superiority of the proposed model to increase the LF. In addition, it is observed from Fig. 2 that scenario 11 has the largest value of VSM in both cases because in this scenario electric demand is at minimum value and the potential of wind power generation is at its maximum value. In contrast, scenario 18 has the lowest value of VSM in both cases because load is at its maximum and the potential of wind power generation is at its minimum. It is also construed from Fig. 2 that in some scenarios (9 and 12) the amount of LF in case (b) is slightly larger than that in case (a).

To observe the effect of different power factors on the LF and planning results, the reactive power at load buses is multiplied by 2.5. Optimal solutions are reported in Table 2, where the results reveal that LF is lower than the corresponding values shown in Table 1. It is concluded that reactive power sources must be incorporated into the planning procedure to avoid extra investment costs for lines and wind farms' construction.

The value of LF for different leading and lagging power factors is denoted in Fig. 3. As can be seen in Fig. 3, when the power factor decreases for the inductive load (lagging power factor), the loading factor reduces as well. On the contrary, the LF increases when the power factor decreases for the capacitive load (leading power factor). Notice that the

**TABLE 1. Optimal planning results for cases (a) and (b).**

| | Case (a): Optimal planning results considering voltage stability | Case (b): Optimal planning results ignoring voltage stability |
|---|---|---|
| Location and capacity (MW) of wind farms | 19 (**500 MW**), 23 (**320 MW**), 24 (**470 MW**) | 20 (**486 MW**), 23 (**500 MW**), 24 (**168 MW**) |
| Selected candidate lines (From-To) | (7-10), (11-15), (13-20), (19-21) | (2-7), (20-22) |
| Total cost (\$) = Lines' investment cost + Wind farms' investment cost + Total generation cost | $6.2608 \times 10^8$ = $3.429000 \times 10^7$ + $1.549096 \times 10^8$ + $4.368833 \times 10^8$ | $5.9130 \times 10^8$ = $1.803 \times 10^7$ + $1.385145 \times 10^8$ + $4.347522 \times 10^8$ |
| Expected loading factor (LF) | 0.213 | 0.184 |

**TABLE 2. Optimal planning results for cases (a1) and (b1).**

| | Case ($a_1$): Optimal planning results considering voltage stability with reactive power demand multiplied by 2.5 | Case ($b_1$): Optimal planning results ignoring voltage stability with reactive power demand multiplied by 2.5 |
|---|---|---|
| Location and capacity (MW) of wind farms | 19 (**500 MW**), 23 (**294 MW**), 24 (**500 MW**) | 15 (**121 MW**), 19 (**315 MW**), 20 (**190 MW**), 24 (**500 MW**) |
| Selected candidate lines (From-To) | (2-7), (7-10), (11-15), (13-20), (13-20), (19-21) | (9-10), (11-24), (20-22) |
| Total cost (\$) = Lines' investment cost + Wind farms' | $6.6686 \times 10^8$ = $4.511000 \times 10^7$ + $1.553105 \times 10^8$ + $4.664419 \times 10^8$ | $5.9991 \times 10^8$ = $2.111 \times 10^7$ + $1.352003 \times 10^8$ + $4.435944 \times 10^8$ |
| investment cost + Total generation cost | | |
| Expected loading factor (*LF*) | 0.177 | 0.124 |

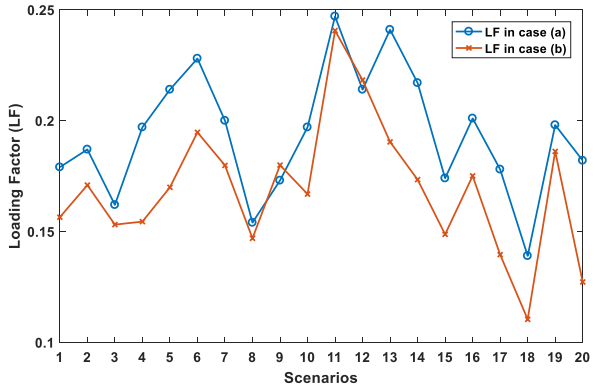


**FIGURE 2.** Loading factors (VSM) for each scenario ($LF_s$).

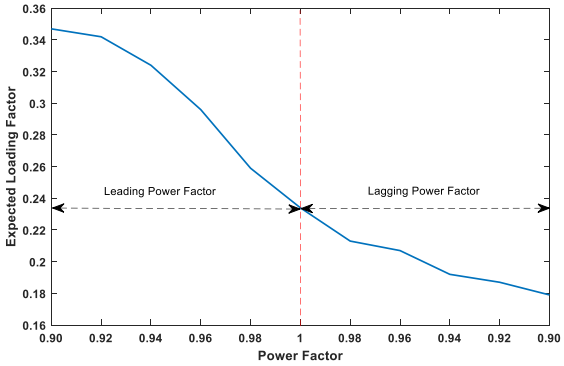


**FIGURE 3.** Expected loading factor (VSM) for different leading and lagging power factor.

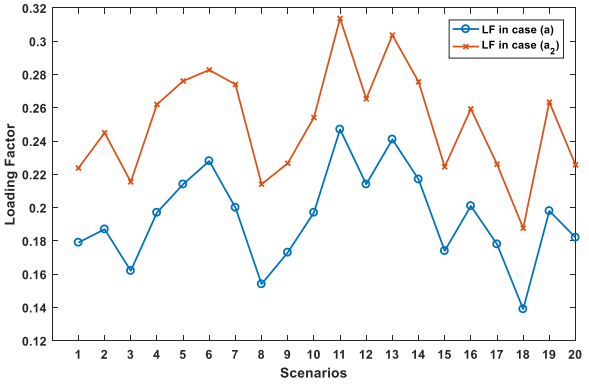


**FIGURE 4.** Loading factor (VSM) with capacitor banks (case (a2)) and without capacitor banks (case (a)).

maximum LF will be about 0.35, and reducing the power factor will not lead to a further increase in the LF. This happens because the thermal capacity of transmission lines has been reached before the voltage collapse occurs.

To improve the LF, five capacitor banks are installed at buses 4, 5, 8, 19, and 20 (case ($a_2$)). These are the buses where voltage collapse occurs when the active and reactive power demand increases. The size of each capacitor bank is considered to be 30 MVar. Comparing the results with case (a) reveals that the total cost is decreased by 9% while the LF is

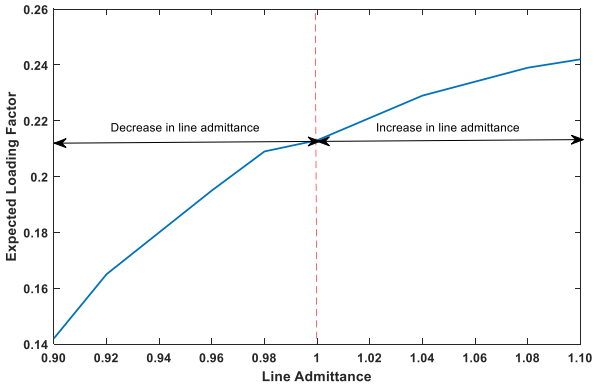


**FIGURE 5.** Expected loading factor (VSM) versus different lines admittance.

increased by 31%. The LF for each scenario with capacitor banks (case ($a_2$)) and without capacitor banks (case (a)) are shown in Fig. 4. As expected, the curve of case ($a_2$) is above the curve of case (a) meaning that effectively-installed reactive power sources can enhance the voltage stability.

To further explore the presented model, the effect of changes in line admittance on the results is investigated. In this regard, Fig. 5 illustrates the LF for different amounts of changes in line admittance. It is observed that as the line admittance increases, the expected LF increases as well. Conversely, when the admittance of the transmission line decreases, the expected LF is significantly reduced. This means using a series compensator can help the system planner enhance the power grid's security.

## V. CONCLUSION

Voltage stability continues to be a vital concern for power grids. In this respect, this paper proposes a novel scheme for transmission expansion planning considering the voltage stability assessment of a power grid embedded with wind power plants under uncertainty. This problem forms a bi-level structure, where the first level identifies the optimal investment model for transmission network and wind farms, and the second level computes the VSM. We use the primal-dual formulation to obtain the optimal solution to this problem. The following concluding remarks are construed from the simulation study:

1- The presented model can effectively improve the VSM. However, the system planner incurs additional costs to enhance the system's voltage stability.
2- The power factor can significantly affect the amount of LF. For lagging (leading) power factor, the LF decreases (increases) by a decrease in power factor.
3- Installing capacitor banks at efficient locations can lead to a reduction in investment costs while improving the system loadability at the same time.
4- The admittance of the transmission lines plays a crucial role in the amount of LF. As the admittance of lines increases, the expected LF grows as well. This means

using a series compensator can help the system planner enhance the power grid's security.

Including several control devices such as capacitors, tap changers, FACTS, and contingency analysis will be a research direction of future work that can be optimized to enhance the VSM.

## ACKNOWLEDGMENT

The authors extend their appreciation to the Deputyship for Research & Innovation, Ministry of Education in Saudi Arabia for funding this research work through the project no. (IFKSURG-2-1587).

## REFERENCES

[1] Y. Yang, S. Lin, Q. Wang, Y. Xie, M. Liu, and Q. Li, "Optimization of static voltage stability margin considering uncertainties of wind power generation," *IEEE Trans. Power Syst.*, vol. 37, no. 6, pp. 4525–4540, Nov. 2022.

[2] Q. Wang, S. Lin, H. B. Gooi, Y. Yang, W. Liu, and M. Liu, "Calculation of static voltage stability margin under N-1 contingency based on holomorphic embedding and Pade approximation methods," *Int. J. Electr. Power Energy Syst.*, vol. 142, Nov. 2022, Art. no. 108358.

[3] *10 Years, Progress to Action*, International Renewable Energy Agency (IRENA), Masdar City, United Arab Emirates, 2020.

[4] P. Vilaça Gomes, J. T. Saraiva, L. Carvalho, B. Dias, and L. W. Oliveira, "Impact of decision-making models in transmission expansion planning considering large shares of renewable energy sources," *Electr. Power Syst. Res.*, vol. 174, Sep. 2019, Art. no. 105852.

[5] Z. Yuan, W. Wang, H. Wang, and N. Ghadimi, "Probabilistic decomposition-based security constrained transmission expansion planning incorporating distributed series reactor," *IET Gener., Transmiss. Distrib.*, vol. 14, no. 17, pp. 3478–3487, Sep. 2020.

[6] K. Meng, W. Zhang, J. Qiu, Y. Zheng, and Z. Y. Dong, "Offshore transmission network planning for wind integration considering AC and DC transmission options," *IEEE Trans. Power Syst.*, vol. 34, no. 6, pp. 4258–4268, Nov. 2019.

[7] C. Zhang, H. Cheng, L. Liu, H. Zhang, X. Zhang, and G. Li, "Coordination planning of wind farm, energy storage and transmission network with high-penetration renewable energy," *Int. J. Electr. Power Energy Syst.*, vol. 120, Sep. 2020, Art. no. 105944.

[8] S. L. Gbadamosi and N. I. Nwulu, "A multi-period composite generation and transmission expansion planning model incorporating renewable energy sources and demand response," *Sustain. Energy Technol. Assessments*, vol. 39, Jun. 2020, Art. no. 100726.

[9] J. Zhan, W. Liu, and C. Y. Chung, "Stochastic transmission expansion planning considering uncertain dynamic thermal rating of overhead lines," *IEEE Trans. Power Syst.*, vol. 34, no. 1, pp. 432–443, Jan. 2019.

[10] M. Moradi-Sepahvand and T. Amraee, "Hybrid AC/DC transmission expansion planning considering HVAC to HVDC conversion under renewable penetration," *IEEE Trans. Power Syst.*, vol. 36, no. 1, pp. 579–591, Jan. 2021.

[11] A. Arabpour, M. R. Besmi, and P. Maghouli, "Transmission expansion and reactive power planning considering wind energy investment using a linearized AC model," *J. Electr. Eng. Technol.*, vol. 14, no. 3, pp. 1035–1043, May 2019.

[12] S. L. Gbadamosi, N. I. Nwulu, and Y. Sun, "Multi-objective optimisation for composite generation and transmission expansion planning considering offshore wind power and feed-in tariffs," *IET Renew. Power Gener.*, vol. 12, no. 14, pp. 1687–1697, Oct. 2018.

[13] S. Zolfaghari Moghaddam, "Generation and transmission expansion planning with high penetration of wind farms considering spatial distribution of wind speed," *Int. J. Electr. Power Energy Syst.*, vol. 106, pp. 232–241, Mar. 2019.

[14] W. Gan, X. Ai, J. Fang, W. Yao, W. Zuo, J. Wen, and M. Yan, "Security constrained co-planning of transmission expansion and energy storage," *Appl. Energy*, vol. 239, pp. 383–394, Apr. 2019.

[15] S. Das, A. Verma, and P. R. Bijwe, "Security constrained AC transmission network expansion planning," *Electr. Power Syst. Res.*, vol. 172, pp. 277–289, Jul. 2019.

[16] Z. Liang, H. Chen, S. Chen, Z. Lin, and C. Kang, "Probability-driven transmission expansion planning with high-penetration renewable power generation: A case study in northwestern China," *Appl. Energy*, vol. 255, Dec. 2019, Art. no. 113610.

[17] S. Wang, G. Geng, and Q. Jiang, "Robust co-planning of energy storage and transmission line with mixed integer recourse," *IEEE Trans. Power Syst.*, vol. 34, no. 6, pp. 4728–4738, Nov. 2019.

[18] G. B. Mir and E. Karatepe, "Stochastic AC transmission expansion planning: A chance constrained distributed slack bus approach with wind uncertainty," *IEEE Access*, vol. 10, pp. 56796–56812, 2022.

[19] A. Almalaq, K. Alqunun, M. M. Refaat, A. Farah, F. Benabdallah, Z. M. Ali, and S. H. E. A. Aleem, "Towards increasing hosting capacity of modern power systems through generation and transmission expansion planning," *Sustainability*, vol. 14, no. 5, p. 2998, Mar. 2022.

[20] B. Chen, T. Liu, X. Liu, C. He, L. Nan, L. Wu, and X. Su, "Distributionally robust coordinated expansion planning for generation, transmission, and demand side resources considering the benefits of concentrating solar power plants," *IEEE Trans. Power Syst.*, early access, May 5, 2022, doi: 10.1109/TPWRS.2022.3171515.

[21] C. A. Moraes, L. W. de Oliveira, E. J. de Oliveira, D. F. Botelho, A. N. de Paula, and M. F. Pinto, "A probabilistic approach to assess the impact of wind power generation in transmission network expansion planning," *Electr. Eng.*, vol. 104, no. 2, pp. 1029–1040, Apr. 2022.

[22] M. A. El-Meligy, A. M. El-Sherbeeny, A. T. A. Soliman, A. E. E. A. Elgawad, and E. A. Naser, "On the solution of robust transmission expansion planning using duality theorem under polyhedral uncertainty set," *Electr. Power Syst. Res.*, vol. 206, May 2022, Art. no. 107785.

[23] C. Li, A. J. Conejo, P. Liu, B. P. Omell, J. D. Siirola, and I. E. Grossmann, "Mixed-integer linear programming models and algorithms for generation and transmission expansion planning of power systems," *Eur. J. Oper. Res.*, vol. 297, no. 3, pp. 1071–1082, Mar. 2022.

[24] Z. Luburic, H. Pandzic, and M. Carrion, "Transmission expansion planning model considering battery energy storage, TCSC and lines using AC OPF," *IEEE Access*, vol. 8, pp. 203429–203439, 2020.

[25] P. F. S. Freitas, L. H. Macedo, and R. Romero, "A strategy for transmission network expansion planning considering multiple generation scenarios," *Electr. Power Syst. Res.*, vol. 172, pp. 22–31, Jul. 2019.

[26] G. Gutiérrez-Alcaraz, N. González-Cabrera, and E. Gil, "An efficient method for contingency-constrained transmission expansion planning," *Electr. Power Syst. Res.*, vol. 182, May 2020, Art. no. 106208.

[27] M. Chen, C. Gao, Z. Li, M. Shahidehpour, Q. Zhou, S. Chen, and J. Yang, "Aggregated model of data network for the provision of demand response in generation and transmission expansion planning," *IEEE Trans. Smart Grid*, vol. 12, no. 1, pp. 512–523, Jan. 2021.

[28] S. Dehghan and N. Amjady, "Robust transmission and energy storage expansion planning in wind farm-integrated power systems considering transmission switching," *IEEE Trans. Sustain. Energy*, vol. 7, no. 2, pp. 765–774, Apr. 2016.

[29] Z. Liang, H. Chen, S. Chen, Y. Wang, C. Zhang, and C. Kang, "Robust transmission expansion planning based on adaptive uncertainty set optimization under high-penetration wind power generation," *IEEE Trans. Power Syst.*, vol. 36, no. 4, pp. 2798–2814, Jul. 2021.

[30] M. O. N. Teixeira, I. D. Melo, and J. A. P. Filho, "An optimisation model based approach for power systems voltage stability and harmonic analysis," *Electr. Power Syst. Res.*, vol. 199, Oct. 2021, Art. no. 107462.

[31] L. Rodriguez-Garcia, S. Perez-Londono, and J. Mora-Florez, "An optimization-based approach for load modelling dependent voltage stability analysis," *Electr. Power Syst. Res.*, vol. 177, Dec. 2019, Art. no. 105960.

[32] B. Gao, G. K. Morison, and P. Kundur, "Voltage stability evaluation using modal analysis," *IEEE Trans. Power Syst.*, vol. 7, no. 4, pp. 1529–1542, Nov. 1992.

[33] S. Liu, R. Shi, T. Zhang, F. Tang, L. Zhang, L. Liu, D. Mao, Z. Li, X. Li, J. Cheng, G. Yan, L. Liu, D. Li, S. Liao, and M. Zhang, "An integrated scheme for static voltage stability assessment based on correlation detection and random bits forest," *Int. J. Electr. Power Energy Syst.*, vol. 130, Sep. 2021, Art. no. 106898.

[34] M. Banejad, M. Kazeminejad, and N. Hosseinzadeh, "Three-phase voltage stability analysis in an integrated transmission-distribution network," *Electr. Power Syst. Res.*, vol. 208, Jul. 2022, Art. no. 107926.

[35] R.-A. Moradi and R. Z. Davarani, "Introducing a new index to investigate voltage stability of power systems under actual operating conditions," *Int. J. Electr. Power Energy Syst.*, vol. 136, Mar. 2022, Art. no. 107637.
[36] Y. Yang, S. Lin, Q. Wang, Y. Xie, and M. Liu, "Multi-objective optimal control approach for static voltage stability of power system considering interval uncertainty of the wind farm output," *IEEE Access*, vol. 8, pp. 119221–119235, 2020.
[37] H. Zhang, G. T. Heydt, and V. Vittal, "An improved network model for transmission expansion planning considering reactive power and network losses," *IEEE Trans. Power Syst.*, vol. 28, no. 3, pp. 3471–3479, Aug. 2013.
[38] Gurobi Optimization. *Gurobi Optimizer Reference Manual*. [Online]. Available: http://www.gurobi.com
[39] G. U. Guide, *GAMS Development Corporation*. Washington DC, USA, 2014.
[40] M. A. Elmeligy. *Data for: A Joint Optimization Model for Transmission Capacity and Wind Power Investment Considering System Security*. [Online]. Available: https://drive.google.com/file/d/1LZs9iJtlKZ_hLRDVbJ8Yj7YRUl0n-snn/view?usp=sharing

**AHMAD M. ALSHAMRANI** received the Ph.D. degree in operations research from Case Western Reserve University, USA. He is currently an Associate Professor with the Department of Statistics and Operations Research, King Saud University, where he worked as the Department Head for eight years. He has done administrative and consultations work for many organizations. His research interests include mathematical programming, inventory, and optimization in general.

**MOHAMMED A. EL-MELIGY** received the B.Sc. degree in information technology from Menoufia University, Egypt, in 2005. He has been a Software Engineer with King Saud University, Riyadh, Saudi Arabia, since 2009. His research interests include petri nets, supervisory control of discrete event systems, database software, and network administration.

**MOHAMED ABDEL FATTAH SHARAF** received the Ph.D. degree in industrial engineering from Chiba University, Japan. He is currently the Head of the Development and Quality Unit, College of Engineering, King Saud University. He has published more than 30 articles in the areas of spare parts control, quality management, maintenance, six-sigma methodology, and academic accreditation.

**EMAD ABOUEL NASR** received the Ph.D. degree in industrial engineering from the University of Houston, Houston, TX, USA, in 2005. He is currently a Professor with the Industrial Engineering Department, College of Engineering, King Saud University, Saudi Arabia, and an Associate Professor with the Mechanical Engineering Department, Faculty of Engineering, Helwan University, Egypt. His current research interests include CAD, CAM, rapid prototyping, advanced manufacturing systems, and collaborative engineering.